

江南造山带西段新元古代超基性岩体年代学 和岩石地球化学研究及其对源区的约束

寇彩化¹, 刘燕学¹, 李廷栋¹, 何万双², 张 恒¹, 丁孝忠¹, 陆济璞³

(1. 中国地质科学院地质研究所, 北京 100037; 2. 中国人民解放军 66259 部队, 内蒙古 呼和浩特 010010;
3. 广西壮族自治区地质调查院, 广西 桂林 541000)

摘要: 本文研究对象为江南造山带西段湘西通道地区长界橄榄辉石岩。长界橄榄辉石岩 LA ICP-MS U-Pb 加权平均年龄为 701 ± 11 Ma。长界橄榄辉石岩主要由单斜辉石、橄榄石和少量斜长石以及少量铁钛氧化物组成, 指示在岩浆形成过程中单斜辉石、橄榄石和少量斜长石为主要分离结晶相。全岩具有低 SiO_2 (44.01%~47.72%)、 Al_2O_3 (6.77%~9.10%)、 TiO_2 (0.49%~0.75%)和全碱($\text{Na}_2\text{O} + \text{K}_2\text{O} = 0.07\% \sim 2.04\%$)含量, 而高 MgO (23.97%~30.70%)含量的特征, 岩石属于亚碱性拉斑玄武岩系列。长界橄榄辉石岩稀土元素总量(ΣREE)较低, 为 $25.7 \times 10^{-6} \sim 55.6 \times 10^{-6}$, 全岩稀土和微量元素标准化图解与洋岛玄武岩(OIB)相似, 具有富集轻稀土元素[(La/Yb)_N 为 3.36~6.48]和富集大离子亲石元素(LILE)的特点, 同时还显示出“弧岩浆”的地球化学性质, 明显的 Nb-Ta 负异常, 较高的 Th/Nb 值(0.52~0.81)和较低的 Nb/La 值(0.25~0.44)以及低 Nb($1.11 \times 10^{-6} \sim 3.91 \times 10^{-6}$)的特征。长界橄榄辉石岩具有高初始($^{87}\text{Sr}/^{86}\text{Sr}$)_i 值(0.707 206~0.708 561)和正的 $\epsilon\text{Nd}(t)$ 值(0.25~0.41)。微量元素模拟结果表明, 长界橄榄辉石岩起源于尖晶石相, 其源区为受来自俯冲消减板片脱水或熔融形成的流体或熔体的交代的软流圈地幔, 是软流圈地幔上涌并发生低度部分熔融的产物(4%~7%)。结合区域地质特征, 推测长界橄榄辉石岩的形成可能与 700 Ma 时期江南造山带西段裂谷作用导致软流圈物质上涌并发生熔融有关。

关键词: 湘西通道地区; 长界橄榄辉石岩; 锆石定年; 软流圈上涌; 裂谷作用

中图分类号: P597⁺.3; P588.12⁺5

文献标识码: A

文章编号: 1000-6524(2016)06-0947-18

Geochronology and geochemistry of Neoproterozoic ultrabasic rocks in the western segment of Jiangnan orogenic belt and constraints on their sources

KOU Cai-hua¹, LIU Yan-xue¹, LI Ting-dong¹, HE Wan-shuang², ZHANG Heng¹, DING Xiao-zhong¹
and LU Ji-pu³

(1. Institute of Geology, Chinese Academy of Geological Sciences, Beijing 100037, China; 2. 66259 Troops of Chinese People's Liberation Army, Hohhot 010010, China; 3. Guangxi Institute of Regional Geological Survey, Guilin 541000, China)

Abstract: This paper reports the characteristics of the Changjie olivine pyroxenolite from the Tongdao area in western Hunan Province, western segment of Jiangnan orogenic belt. Laser ablation inductively coupled plasma mass spectrometry (LA ICP-MS) U-Pb zircon dating of the Changjie olivine pyroxenolite yielded an age of 701 ± 11 Ma. The Changjie olivine pyroxenolite contains clinopyroxene, olivine and plagioclase together with a small amount of Fe-Ti oxide minerals, probably suggesting that clinopyroxene, olivine and plagioclase fractionated within the magma chamber. Geochemically, the Changjie olivine pyroxenolite is characterized by relatively low

收稿日期: 2016-05-31; 接受日期: 2016-10-17

基金项目: 国家自然科学基金资助项目(41402052); 中国地质调查资助项目(1212011120117, 1212011120115)

作者简介: 寇彩化(1985-), 女, 助理研究员, 博士, 主要从事岩石地球化学研究, E-mail: caihuakou@163.com.

SiO_2 (44.01%~47.72%), Al_2O_3 (6.77%~9.10%), TiO_2 (0.49%~0.75%), and total alkali ($\text{Na}_2\text{O} + \text{K}_2\text{O}$ =0.07%~2.04%), and high MgO (23.97%~30.70%) content, and these rocks are of tholeiitic series and belong to sub-alkali series. These rocks display ocean island basalt (OIB)-like signatures, characterized by the enrichment of light rare earth elements [LREE, $(\text{La}/\text{Yb})_{\text{N}} = 3.36 \sim 6.48$] and large ion lithophile elements (LILE) relative to high rare earth elements (HREE). Moreover, they also display typical arc magma features, such as significant Nb-Ta troughs, relatively high Th/Nb ratios (0.52~0.81) and low Nb/La (0.25~0.44) ratios, and typical low Nb content ($1.11 \times 10^{-6} \sim 3.91 \times 10^{-6}$). These rocks show relatively high initial ($^{87}\text{Sr}/^{86}\text{Sr}$)_i ratios (0.707 206~0.708 561) and positive $\epsilon\text{Nd}(t)$ values (0.25~0.41). Furthermore, the geochemical signature also suggests that the Changjie olivine pyroxenolite was produced by low degree of partial melting (4%~7%) of the spinel-facies, asthenospheric mantle peridotite which had been matasomatized by slab-derived fruits/melts. In combination with the regional geology, the authors infer that the deep dynamic mechanism for the formation of the Changjie olivine pyroxenolite was related to the partial melting of upwelling asthenosphere mantle due to the rifting at about 700 Ma in the western segment of Jiangnan orogenic belt.

Key words: Tongdao area in western Hunan Province; Changjie olivine pyroxenolite; zircon geochronology; upwelling asthenosphere; rifting

Fund support: Project of Natural Science Foundation of China (41402052); China Geological Survey (1212011120117, 1212011120115)

位于华南的江南造山带是 Rodinia 超大陆聚合背景下扬子板块与华夏板块历经洋壳俯冲、弧-陆碰撞以及陆-陆碰撞等多期构造运动的产物(如, 夏斌, 1984; 郭令智等, 1996; Li, 1999; Zhao and Cawood, 1999; Li *et al.*, 1999, 2003a, 2003b, 2009, 2010; Wu *et al.*, 2006; Wang *et al.*, 2008, 2014; Zheng *et al.*, 2008; Zhang *et al.*, 2008; Zhou *et al.*, 2009; Faure *et al.*, 2009; Shu *et al.*, 2011)。一直以来是学界研究的热点及重点地区。对江南造山带构造岩浆活动的研究,对于认识 Rodinia 超大陆演化具有重要意义。江南造山带构造岩浆活动非常复杂,前人对江南造山带西段新元古代岩浆岩的成因机制做了详细的研究,并取得了一些认识,目前主要有以下3种观点:①部分学者指出这些岩石形成时代多集中在854~760 Ma时期,且具有弧岩浆的特征,因而他们认为该时期江南造山带西段处于吉华南洋板片北西向俯冲于扬子板块之下的构造背景(Yan *et al.*, 2004; Zhou *et al.*, 2004, 2009; Yao *et al.*, 2013, 2014);②部分学者通过对江南造山带西段新元古代岩浆岩研究,如桂北828 Ma时期的辉长岩和桂北820 Ma时期的S型花岗岩(Li, 1999; Li *et al.*, 1999, 2003a, 2003b, 2010)以及桂北和湘西760 Ma时期的基性-超基性岩(周继彬, 2006; Zhou *et al.*, 2007; 张春红等, 2009),指出该区在825 Ma和760 Ma时期存在地幔柱活动,即该区处于地幔柱

活动所致的大陆裂谷伸展背景;③还有学者通过对江南造山带西段基性岩体和S型花岗岩的年代学和地球化学研究,认为835~800 Ma期间,江南造山带西段进入了后碰撞拉张构造背景阶段,即江南造山带西段在该时期处于俯冲板片断离的构造背景(Wang *et al.*, 2004, 2006, 2008, 2014)。上述学者从不同角度对江南造山带西段在850~760 Ma时期的构造演化开展了有益的探讨,但对于此后江南造山带西段(即760~700 Ma期间,尤其700 Ma时期)的研究则较为薄弱。Druschke等(2006)通过对扬子板块北缘和西缘地层学和碎屑锆石年代学的研究,初步判断江南造山带西段在850~700 Ma时期处于俯冲的构造环境;另有部分学者则认为在~700 Ma时期江南造山带西段处于裂谷背景下(陆松年, 2001; 王孝磊等, 2003; 舒良树, 2012)。遗憾的是,上述研究都缺少岩石学和年代学证据,目前见诸报道的仅有湖南中部高桥地区的震旦纪玄武岩(王孝磊等, 2003)。可见,前人虽然对江南造山带西段构造演化做了较为详细的研究,但仍有一些重要的科学问题亟待解决。

本文对新近发现于江南造山带西段湘西通道地区的小规模超基性岩开展了系统的岩石学、年代学、元素和同位素地球化学研究。本次研究厘定其成岩时代约为700 Ma,认为其源区为受到俯冲熔体/流体交代的软流圈地幔。结合前人的研究成果,初步

探讨了江南造山带西段在 700 Ma 时期的深部动力学过程,从而完善了对江南造山带西段 700 Ma 时期构造演化背景的认识,也为 Rodinia 超大陆裂解提供了重要的依据。

1 地质背景及岩石学特征

以江绍断裂为界,华南地区被划分为扬子板块和华夏板块两个构造单元(图 1)。扬子板块出露的最古老岩石单元为崆岭群杂岩($\sim 3.2\sim 2.0$ Ga),主

要由太古代-早元古代高级变质英云闪长岩、奥长花岗岩、花岗闪长片麻岩和角闪岩等组成(Gao *et al.*, 1999),华夏板块最古老的岩石为浙东南闽西北地区的八都群(Yu *et al.*, 2009)。伴随着古华南洋的闭合,扬子板块与华夏板块在新元古代时期(1.0~0.8 Ga)历经洋壳俯冲、弧-陆碰撞以及陆-陆碰撞等构造运动(即“四堡运动”),形成了江南造山带(夏斌, 1984; Li *et al.*, 1995; 郭令智等, 1996; 葛文春等, 2001; 胡受奚等, 2006; 薛怀民等, 2010; Shu *et al.*, 2011; 舒良树, 2012; Zhong *et al.*, 2016)(图 1)。

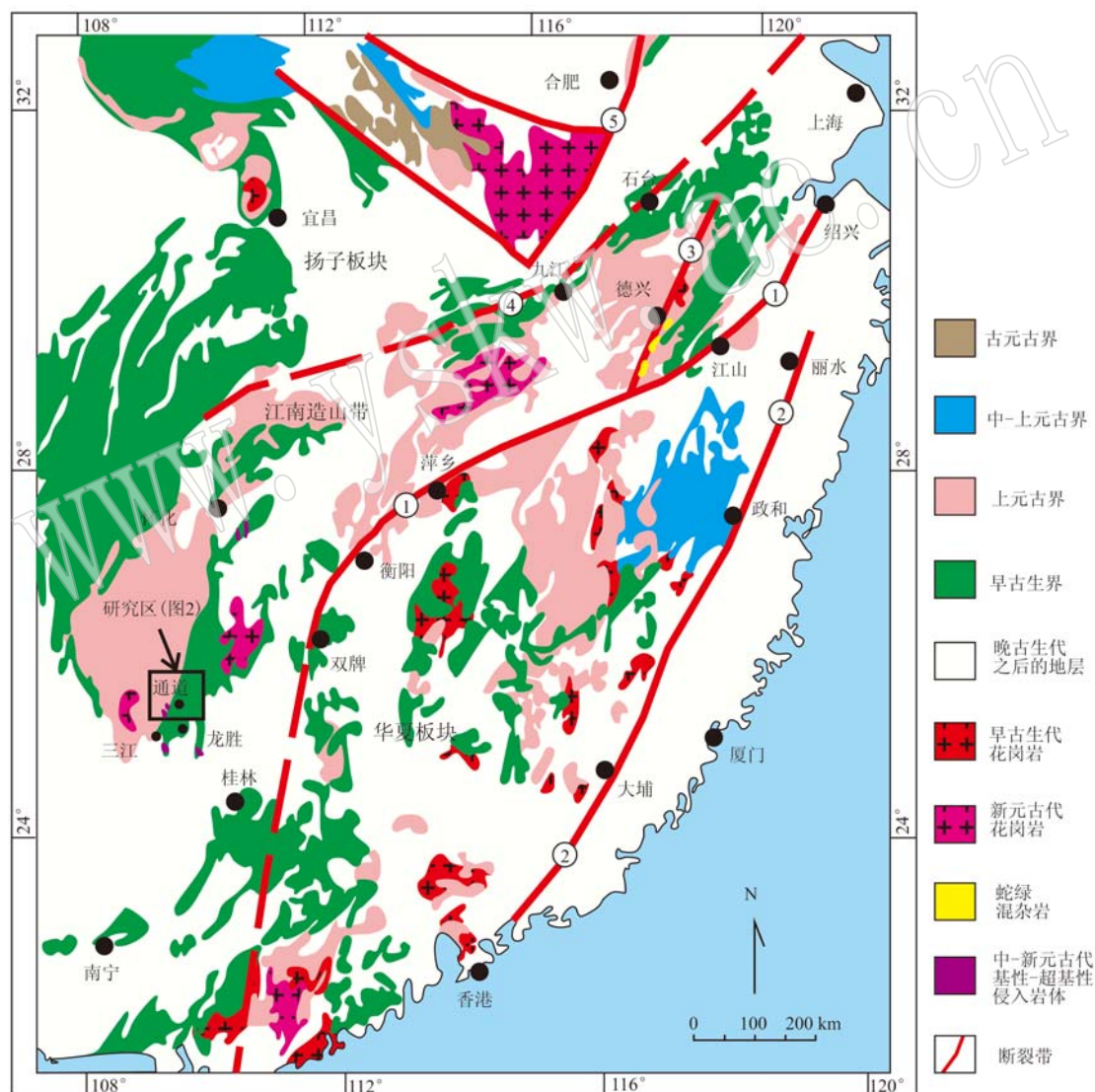


图 1 江南造山带地质示意简图(据 Yao *et al.*, 2014)

Fig. 1 Geological sketch map of the Jiangnan orogenic belt (modified after Yao *et al.*, 2014)

①—绍兴-江山-萍乡-双牌断裂; ②—政和-大埔断裂; ③—赣东北断裂; ④—九江-石台断裂; ⑤—郯庐断裂

①—Shaoxing-Jiangshan-Pingxiang-Shuangpai fault; ②—Zhenghe-Dapu fault; ③—Northeast Jiangxi fault; ④—Juijiang-Shitai fault;

⑤—Tanlu fault

江南造山带呈 NEE 方向展布, 西起黔东、桂北, 经湘西北、赣西北、赣东北, 东至皖南、浙西, 长约 1 500 km、宽约 200 km, 面积约 30 万平方公里(郭令智等, 1980, 1996)。造山带东段主要位于赣东北、皖南、浙西、浙东北等地区, 西段位于桂北和湖南以及贵州等地区(Yao et al., 2014)(图 1)。江南造山带西段湘西地区出露的最古老地层为中元古界冷家溪群, 其次为角度不整合于其上的上元古界板溪群。其中, 冷家溪群为一套浅灰-浅灰绿色浅变质细粒碎屑岩、粘土岩, 局部夹基性-中酸性火山岩, 其中的斑脱岩 SHRIMP 锆石 U-Pb 年龄为 822 Ma(高林志等, 2011); 板溪群由下部的合桐组和上部的拱洞组组成(图 2a), 其岩性主要为浅变质砂砾岩、长石石英砂岩、板岩及凝灰岩, 局部夹基性-中酸性火山岩, 高林志等(2011)获得其下部斑脱岩 SHRIMP 锆石 U-Pb

年龄为 802 Ma。本区还出露有南华系、寒武系和泥盆系地层(图 2a)。江南造山带西段构造岩浆活动复杂, 中酸性和基性-超基性岩浆岩均较为发育, 且大都形成于 850~770 Ma 之间(Li, 1999; Zhou et al., 2004, 2007, 2009; Yan et al., 2004; Yao et al., 2013, 2014)。其中, 酸性岩主要以 S 型花岗岩为主, 如 819 ± 9 Ma 的四堡花岗岩和 824 ± 4 Ma 的三防花岗岩体等(Li, 1999; Li et al., 1999, 2003a, 2003b, 2010); 基性-超基性岩石在江南造山带西段湘西-桂北地方均有出露, 主要以岩脉岩墙形式产出, 如震旦纪湖南中部高桥玄武岩(王孝磊等, 2003), 形成于约 760 Ma 的桂北龙胜辉长岩(葛文春等, 2001)、768 Ma 的湘西古丈辉绿岩(周继彬, 2006)、825 Ma 的桂北元宝山地区超基性岩石(周继彬, 2006)以及 830 Ma 的湘西隘口辉橄岩(张春红等, 2009)等。

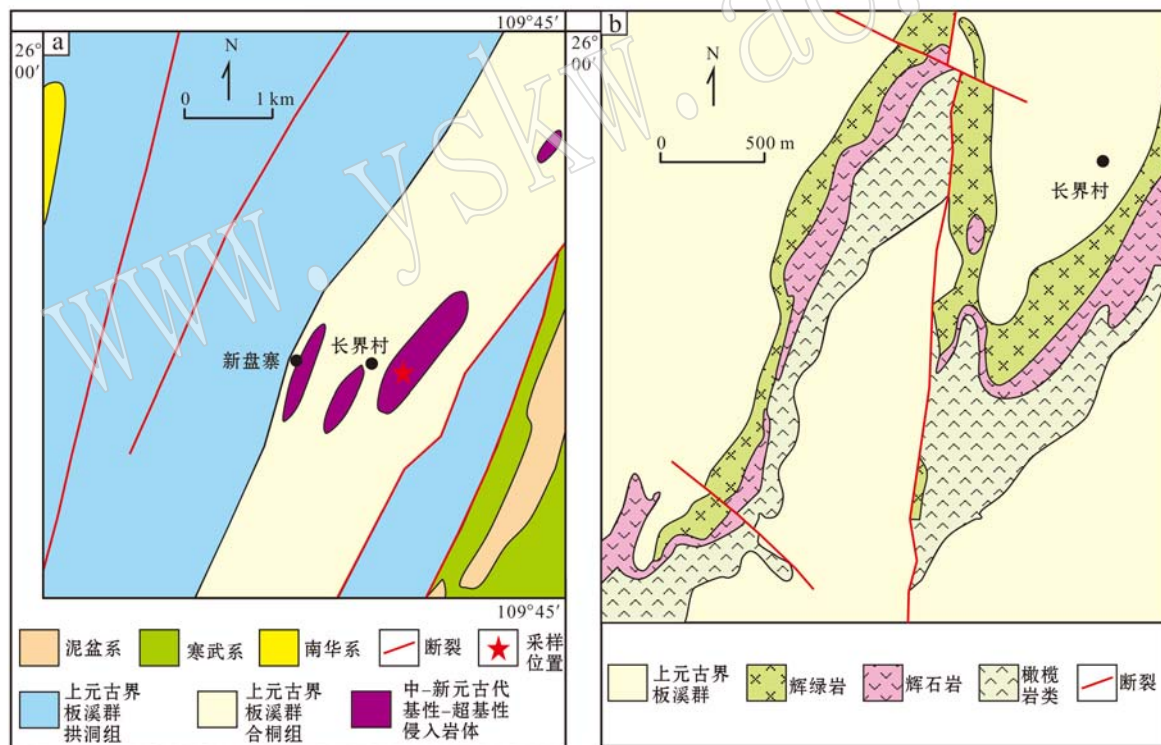


图 2 湘西通道长界基性-超基性岩地质图(a 据 1:5 万林溪幅^①, b 据湖南省区域地质志^②)

Fig. 2 Sketch geological map of the mafic-ultramafic rocks (a after 1:50 000 Linxi Geological Map^①, b after Records of Regional Geology of Hunan Province^②)

^① 广西区域地质调查研究院. 2011. 湖南省林溪幅 1:5 万地质草图.

^② 湖南省地质矿产局. 1988. 湖南省区域地质志.

本次研究对象为湘西通道地区长界基性-超基性岩体, 岩石类型主要有辉绿岩、辉长岩、辉石岩和橄榄辉石岩, 这些岩石呈渐变过渡的关系。该地区岩体数量众多, 形态较为稳定, 大多以岩床形式顺层侵入到板溪群合桐组浅变质岩中(图 2a, 2b), 单个岩体一般厚约 10~100 m, 出露面积较小, 多小于 0.1 km²。

本次采集的长界基性-超基性岩主要为橄榄辉

石岩类, 岩石具堆晶结构, 造岩矿物主要为单斜辉石(70%)和橄榄石(25%), 含少量斜长石(5%)。橄榄石呈自形-半自形粒状, 颗粒粒径 0.2~5 mm, 普遍发育蛇纹石化(图 3a); 单斜辉石颗粒粒径约 0.3~5 mm, 呈自形-半自形粒状(图 3b), 部分单斜辉石颗粒裂纹发育(图 3c), 并发育绿帘石、绿泥石化和透闪石化(图 3c, 3d)。副矿物主要有钛铁矿、磁铁矿和黄铁矿, 还含有少量磷灰石、斜锆石、锆石及榍石。

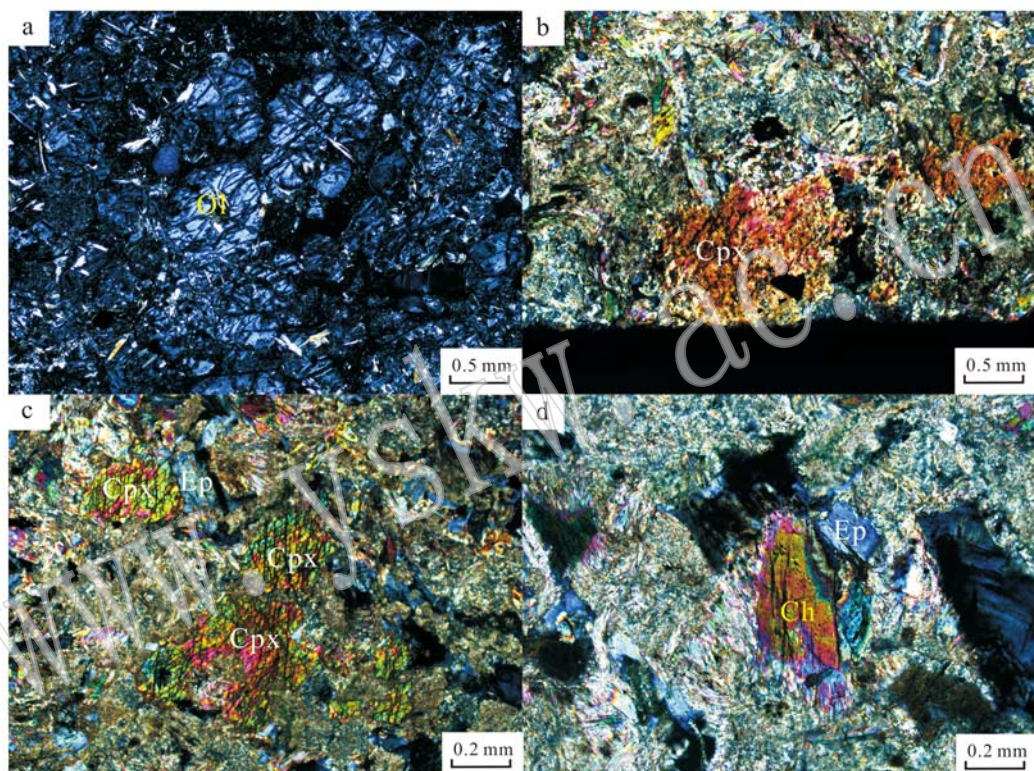


图 3 长界橄榄辉石岩显微镜特征(正交偏光)

Fig. 3 Thin section characteristics of Changjie olivine pyroxenolite (crossed nicols)

Ol—橄榄石; Cpx—单斜辉石; Ep—绿帘石; Ch—绿泥石

Ol—olivine; Cpx—clinopyxene; Ep—epidote; Ch—chlorite

2 分析方法

本文对 1 件橄榄辉石岩样品(CJ14-9)中的锆石进行了 U-Pb 年代学测定, 使用常规的重液浮选和电磁分离方法挑选出锆石颗粒, 随后在双目镜下根据颜色、形态学和透明度等特征进行初步分类, 并挑选出具有代表性的锆石, 将锆石样品分别用双面胶粘贴在载玻片上, 放上 PVC 环, 然后将环氧树脂和固化剂进行充分混合后注入 PVC 环中, 待树脂充分固化后将样

品从载玻片上剥离, 并对其进行抛光, 直到样品露出一个光洁的平面, 并进行锆石阴极发光(CL)照相。样品的 LA ICP-MS U-Pb 定年在武汉上谱科技有限责任公司完成, 实验分析用激光剥蚀系统为 GeoLas Pro, 等离子质谱仪为 Agilent 7700, 激光能量为 80 mJ, 频率为 5 Hz, 激光束斑直径为 32 μm, 具体分析条件及流程见文献 Liu 等(2008, 2010a, 2010b)。年龄计算机谐和图采用 Isoplot(3.0)完成。

对样品在偏光显微镜下进行详细的薄片检查后, 选取 6 件具有代表性且蚀变程度相对较低的样

品进行全岩地球化学分析。所分析样品均是在切除表皮风化物后洗净晾干,在玛瑙乳钵中研磨至200目。主量、稀土和微量元素分析在国家地质实验测试中心完成,其中主量元素分析方法为XRF,稀土和微量元素分析方法为ICP-MS,具体方法可见Qi等(2000)。Rb-Sr和Sm-Nd同位素比值测定在南京大学现代分析中心由英国制造的VG354多接受质谱计上完成,具体方法可见王银喜等(2007)。

3 分析结果

3.1 锆石U-Pb年代学

锆石LA ICP-MS U-Pb分析结果列于表1。如图4a所示,橄榄辉石岩样品中的锆石较少且都较小,多为50~80 μm,呈短柱或长柱状,未见明显震荡环带,锆石的Th/U值为0.48~2.73(表1),暗示这些锆石均为岩浆成因锆石(Hoskin and Schaltegger, 2003; Hoskin, 2005)。本次研究选择相对较大的14颗锆石进行了测试分析。其中,CJ14-9-2、11、12、13四颗锆石的年龄明显较老,可能为捕获锆石,CJ14-9-4、10、14三颗锆石年龄较小,可能是受后期岩浆-热事件影响所形成的锆石,CJ14-9-1、5、6三颗锆石太小而未采集到可用数据(表1)。剔除上述测点后,剩余4个测试点锆石与谐和线的交点为701±16 Ma,其²⁰⁶Pb/²³⁸U的加权平均年龄为701±11 Ma(图4b,4c),二者在误差范围内完全一致,认为该年龄可代表通道长界橄榄辉石岩的成岩年龄。

3.2 全岩主量元素特征

全岩主量元素分析结果列于表2(本文所研究的样品烧失量较高为6.83%~11.78%,所有表2中的主量元素为除烧失量后的结果)。长界橄榄辉石岩具有低SiO₂(44.01%~47.72%)、Al₂O₃(6.77%~9.10%)、TiO₂(0.49%~0.75%)和全碱(Na₂O+K₂O=0.07%~2.04%)含量,而高MgO含量(23.97%~30.70%)的特征。整体上,长界橄榄辉石具有与桂北元宝山地区超基性岩石相似而不同于湘西古丈和通道地区的辉绿岩主量元素地球化学特征,如桂北元宝山地区超基性岩石也具有低SiO₂(37.3%~47.6%)、Al₂O₃(2.0%~5.2%)、TiO₂(0.16%~1.09%)和全碱(Na₂O+K₂O=0.31%~0.67%)含量,而高MgO含量(20.8%~35.6%)的特征(周继彬,2006; Yao et al., 2014),而湘西古丈和通道辉绿岩则具有较高的SiO₂(50.2%~

53.0%)、Al₂O₃(14.8%~17.4%)、TiO₂(1.31%~1.98%)和全碱含量(Na₂O+K₂O=4.9%~6.0%),低MgO含量(6.05%~8.45%)的特征(Zhou et al., 2007)。另外,长界橄榄辉石岩Mg[#](78.0~81.9)高,与桂北元宝山地区超基性岩石Mg[#]相当(76~88)(周继彬,2006; Yao et al., 2014),而明显高于湘西古丈和通道辉绿岩的Mg[#](51~62)(Zhou et al., 2007)。长界橄榄辉石岩属亚碱性系列(图5a),在Zr-Y图解中,这些岩石均落入拉斑玄武岩类范围(图5b)。

3.3 全岩稀土和微量元素特征

全岩稀土和微量元素分析结果列于表2。长界橄榄辉石岩稀土元素总量(Σ REE)较低,为 25.7×10^{-6} ~ 55.6×10^{-6} ,与桂北元宝山地区超基性岩相似(绝大多数样品 Σ REE为 9.5×10^{-6} ~ 53.1×10^{-6} , Yao et al., 2014)。在稀土元素球粒陨石标准化图解中(图6a),所有样品的分配曲线都呈轻稀土富集的右倾型,其(La/Yb)_N值为3.36~6.48,(La/Sm)_N值为1.50~2.67,说明样品的轻重稀土和轻中稀土分异皆较为明显。除两个样品具有弱的Eu正异常外(δ Eu为1.09和1.17),其余样品均具有轻微Eu负异常(δ Eu为0.68~0.89)(表2,图6a)。总体而言,样品具有与洋岛玄武岩(OIB)相似的稀土元素配分模式和微量元素配分曲线,具有富集轻稀土(LREE)和大离子亲石元素(LILE)的特点,而明显不同于大洋中脊玄武岩(MORB)的稀土和微量元素配分模式。但值得注意的是,长界橄榄辉石岩还显示出“弧岩浆”的地球化学性质,如明显的Nb-Ta负异常,较高的Th/Nb值(0.52~0.81)和较低的Nb/La值(0.25~0.44)以及低Nb值(1.11×10^{-6} ~ 3.91×10^{-6})。

3.4 全岩同位素特征

全岩Rb-Sr和Sm-Nd同位素比值分析结果列于表3,初始($^{87}\text{Sr}/^{86}\text{Sr}$)_i同位素比值和 $\epsilon\text{Nd}(t)$ 值以长界橄榄辉石岩的成岩年龄700 Ma计算,从表3可知,所有长界橄榄辉石岩具有相似的Sr-Nd同位素组成。长界橄榄辉石岩具有较高的 $^{87}\text{Rb}/^{86}\text{Sr}$ 值(0.374 6~0.649 3)和初始($^{87}\text{Sr}/^{86}\text{Sr}$)_i值(0.707 206~0.708 561)。长界橄榄辉石岩的 $^{147}\text{Sm}/^{144}\text{Nd}$ 和 $^{143}\text{Nd}/^{144}\text{Nd}$ 值分别为0.141 8~0.169 5和0.512 401~0.512 526, $\epsilon\text{Nd}(t)$ 值为0.25~0.41(图7),明显低于桂北元宝山地区超基性岩石和湘西古丈和通道辉绿岩的 $\epsilon\text{Nd}(t)$ 值(分别为4.01~6.51和2.9~3.3,周继彬,2006)。

表1 湘西通道长界橄榄辉石岩U-Pb锆石年龄
Table 1 U-Pb data for zircons from Changjie olivine pyroxenolite in the Tongdao area in western Hunan Province

样号	同位素比值							表面年龄/Ma								
	$^{207}\text{Pb}/^{206}\text{Pb}$	1σ	$^{207}\text{Pb}/^{235}\text{U}$	1σ	$^{206}\text{Pb}/^{238}\text{U}$	1σ	Pb	Th	U	Th/U	$^{207}\text{Pb}/^{206}\text{Pb}$	1σ	$^{207}\text{Pb}/^{235}\text{U}$	1σ	$^{206}\text{Pb}/^{238}\text{U}$	1σ
CJ14-9-1	0.0975	0.0060	0.8691	0.0505	0.0645	0.0014	921.0	1 961.6	719.8	2.73	1 576	115	635	27.5	403	8.4
CJ14-9-2	0.2508	0.0124	5.3795	0.3553	0.1505	0.0036	2 321.4	1 032.4	715.0	1.44	3 190	78.4	1 882	56.6	904	20.0
CJ14-9-3	0.1352	0.0084	2.1921	0.1512	0.1149	0.0018	399.2	341.4	252.0	1.35	2 169	109	1 179	48.1	701	10.4
CJ14-9-4	0.0553	0.0013	0.5170	0.0127	0.0672	0.0009	375.7	712.2	1 473.6	0.48	433	55.6	423	8.5	419	5.3
CJ14-9-5	0.0788	0.0031	0.8701	0.0340	0.0795	0.0015	847.3	1 647.0	611.2	2.60	1 169	71	636	18.5	493	9.2
CJ14-9-6	0.1087	0.0039	1.4825	0.0567	0.0979	0.0020	812.9	1 078.0	543.5	1.93	1 789	66	923	23.2	602	11.9
CJ14-9-7	0.1400	0.0197	2.1870	0.2807	0.1136	0.0039	843.8	661.4	608.8	1.09	2 227	246	1 177	89.5	693	22.6
CJ14-9-8	0.0733	0.0027	1.1694	0.0428	0.1145	0.0016	1 140.6	1 355.9	901.4	1.50	1 022	74	786	20.1	699	9.0
CJ14-9-9	0.0734	0.0022	1.1789	0.0377	0.1153	0.0019	867.8	1 123.7	567.9	1.98	1 033	59	791	17.6	704	10.9
CJ14-9-10	0.3392	0.1177	0.5373	0.5210	0.0420	0.1472	5 861.3	62.9	25.3	2.49	3 659	559	437	344	265	911
CJ14-9-11	0.1816	0.0254	3.8171	0.4676	0.1718	0.0136	1 371.6	799.7	548.6	1.46	2 668	233	1 596	98.6	1 022	75.1
CJ14-9-12	0.0663	0.0021	1.3174	0.0452	0.1440	0.0025	206.4	223.2	208.7	1.07	815	66.7	853	19.8	867	14.1
CJ14-9-13	0.5087	0.0454	19.4899	3.3567	0.2792	0.0330	581.8	99.4	78.0	1.27	4 333	132	3 066	166	1 587	166
CJ14-9-14	0.0668	0.0020	0.9726	0.0293	0.1049	0.0014	669.0	987.9	655.1	1.51	831	63.0	690	15.1	643	8.1

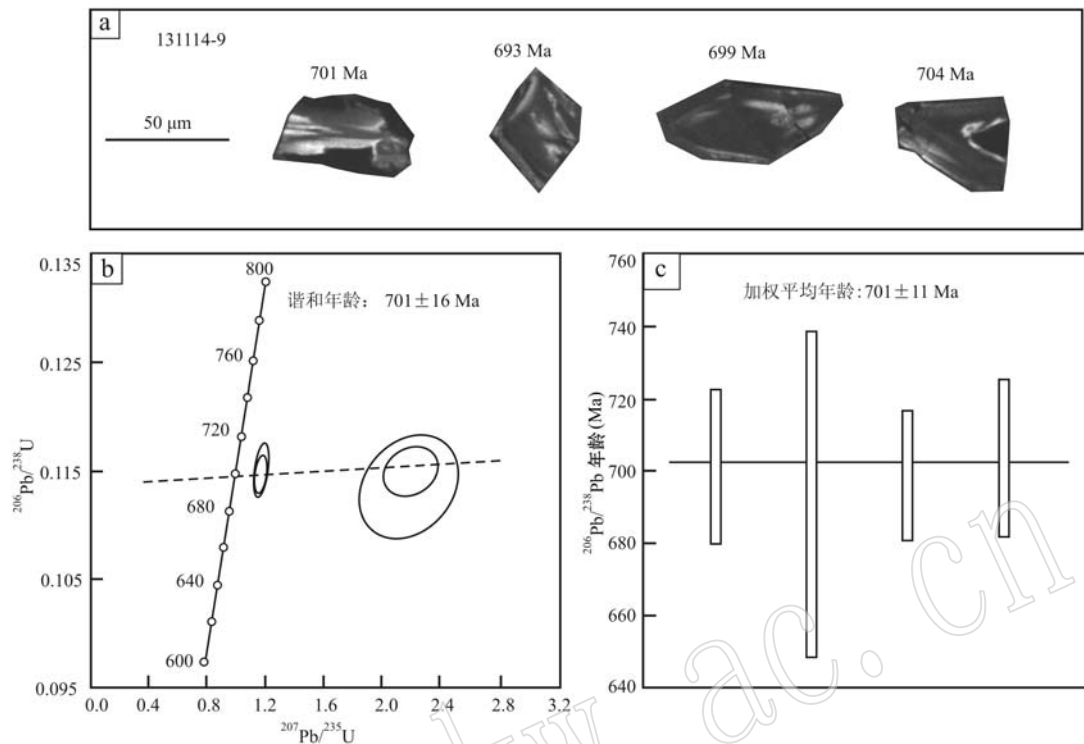


图 4 长界橄榄辉石岩锆石 CL 图像和 U-Pb 谱和图解

Fig. 4 CL image and U-Pb concordia diagrams for zircons from the Changjie olivine pyroxenolite

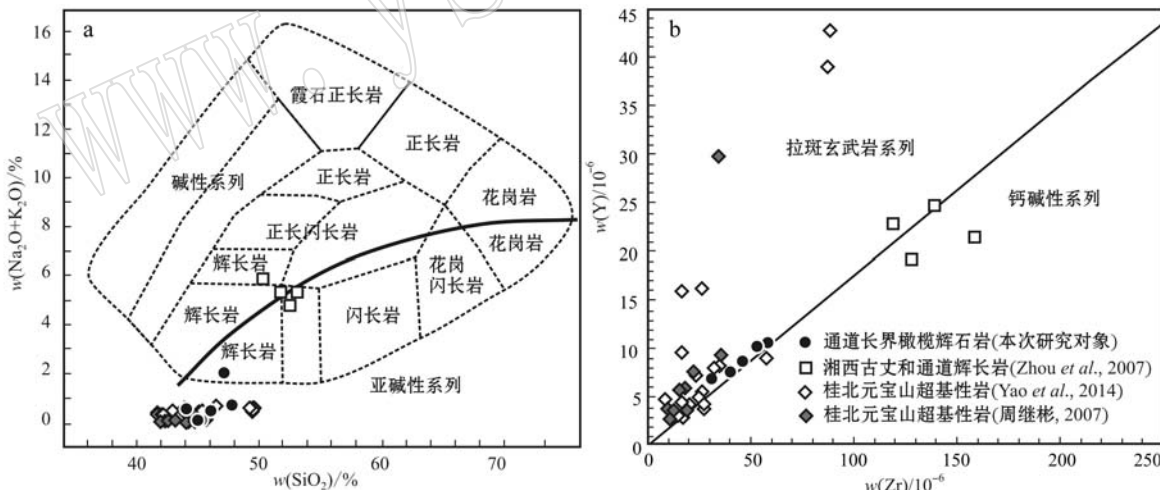


图 5 长界橄榄辉石岩 TAS 图解(a, Wilson, 1989)和 Y-Zr 图解(b, Polat et al., 2009)

Fig. 5 TAS diagram (a, after Wilson, 1989) and Y-Zr variation (b, after Polat et al., 2009) of Changjie olivine pyroxenolite

4 讨论

4.1 分离结晶和地壳混染

4.1.1 分离结晶

长界橄榄辉石岩主要为粒状结构(图 3), 结晶矿

物主要为单斜辉石和橄榄石, 另有少量斜长石, 表明岩浆演化过程中单斜辉石和橄榄石为主要的分离结晶相, 有少量斜长石可能也发生了分离结晶作用。另外, 从主量元素相关性图解(图 8)中可以看出, MgO 与 SiO₂、Al₂O₃、TiO₂、全碱(Na₂O + K₂O) 和 CaO 呈负相关而与 TFe₂O₃ 呈正相关, 同样表明通道

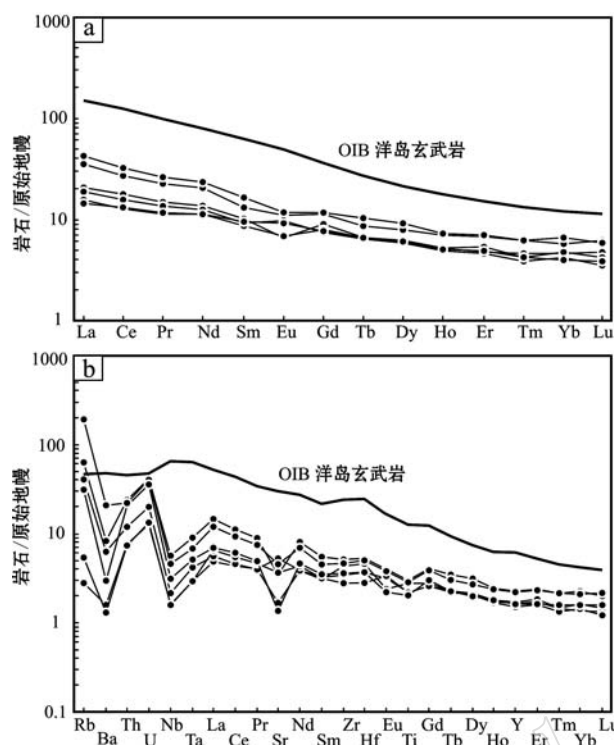


图 6 长界橄榄辉石岩微量元素标准化图解

Fig. 6 Normalized trace element patterns of the Changjie olivine pyroxenolite

标准化数据和 OIB 数据来自 Sun and McDonough(1989)
Normalized values and data of OIB are from Sun and
McDonough (1989)

长界橄榄辉石岩的母岩浆可能发生过单斜辉石和橄榄石的分离结晶。此外, MgO 与微量元素 Ni 和 Cr 的变化关系也指示在岩浆演化的过程中, 发生了单斜辉石和橄榄石以及少量钛铁氧化物的分离结晶, 这与岩相学的观察一致。

4.1.2 地壳混染

长界橄榄辉石岩具有高的初始($^{87}\text{Sr}/^{86}\text{Sr}$)_i值(0.707 206~0.708 561)和低 $\epsilon_{\text{Nd}}(t)$ 值(0.25~0.41)(图 7), 指示其可能受到了地壳物质的混染(Taylor and McLennan, 1985)。微量元素 Th 和 Ta 易受地壳混染作用的影响, 若受地壳混染则会导致 Th/Ta 值升高, 通道橄榄辉石岩 Th/Ta 值为 2.5~4.1, 高于原始地幔的 Th/Ta 值(2.1, Sun and McDonough, 1989), 而接近地壳的 Th/Ta 值(3.5, Taylor and McLennan, 1985), 长界橄榄辉石岩具有高的(Th/Yb)_{PM}值(5.5~12.9)和(La/Nb)_{PM}值(2.4~4.2), 这些特征说明长界橄榄辉石岩可能受到了地壳物质的混染。另外, 受岩石圈地幔物质混染可

表 2 全岩主量元素($w_{\text{B}}/\%$)和微量元素($w_{\text{B}}/10^{-6}$)分析结果

Table 2 Bulk rock composition of major ($w_{\text{B}}/\%$) and trace elements ($w_{\text{B}}/10^{-6}$)

样品号	CJ14-1	CJ14-3	CJ14-4	CJ14-5	CJ14-6	CJ14-7
SiO_2	44.01	44.95	46.05	47.06	47.72	45.12
TiO_2	0.71	0.57	0.49	0.70	0.75	0.54
Al_2O_3	6.90	6.99	9.10	8.43	8.64	6.77
FeO^{T}	13.94	13.86	14.26	13.49	13.99	13.49
MnO	0.26	0.23	0.25	0.25	0.23	0.21
MgO	30.70	29.02	25.37	23.97	24.79	30.59
CaO	2.83	4.25	3.92	3.96	3.05	3.12
Na_2O	0.12	0.03	0.14	0.04	0.04	0.03
K_2O	0.45	0.03	0.33	2.00	0.70	0.06
P_2O_5	0.07	0.06	0.08	0.09	0.09	0.07
$\text{Mg}^{\#}$	81.5	80.7	78.1	78.0	78.0	81.9
LOI	8.67	11.78	6.83	7.30	8.24	10.98
Total	99.34	99.09	98.33	98.39	98.65	99.44
Y	7.86	7.76	7.50	10.20	10.50	6.90
La	3.84	3.47	4.93	8.44	10.30	4.57
Ce	8.14	8.16	11.00	16.80	20.10	9.83
Pr	1.11	1.13	1.40	2.14	2.53	1.30
Nd	5.40	5.44	6.36	9.76	11.20	5.98
Sm	1.37	1.49	1.57	2.07	2.49	1.42
Eu	0.41	0.55	0.38	0.64	0.69	0.57
Gd	1.69	1.59	1.84	2.34	2.47	1.55
Tb	0.25	0.25	0.25	0.33	0.39	0.24
Dy	1.62	1.58	1.51	2.02	2.35	1.52
Ho	0.30	0.29	0.30	0.40	0.41	0.28
Er	0.91	0.83	0.80	1.14	1.17	0.77
Tm	0.11	0.11	0.12	0.16	0.16	0.10
Yb	0.82	0.68	0.79	1.05	1.14	0.72
Lu	0.11	0.10	0.12	0.16	0.15	0.09
Rb	26.60	1.80	20.10	125.00	42.60	3.48
Sr	34.90	113.00	28.50	93.70	72.10	76.70
Ba	43.50	10.90	20.20	145.00	57.10	8.86
Th	1.02	0.64	1.76	1.86	2.04	0.62
U	0.44	0.28	0.77	0.88	0.92	0.29
Nb	1.53	1.11	2.17	3.23	3.91	1.13
Ta	0.17	0.12	0.21	0.28	0.37	0.12
Zr	49.30	39.40	40.60	53.20	58.40	31.30
Hf	1.46	1.17	1.16	1.57	1.65	0.87
Ni	1.469	1.384	623	970	1.028	1.441
Cr	1.948	1.753	1.221	1.478	1.421	1.788
Pb	4.01	1.65	1.29	4.13	11.80	3.33
Ti	3.657	2.896	2.661	3.699	3.901	2.878
(La/Sm) _N	1.81	1.50	2.03	2.63	2.67	2.08
(La/Yb) _N	3.36	3.66	4.48	5.77	6.48	4.55
(Dy/Yb) _N	1.32	1.56	1.28	1.29	1.38	1.41
δEu	0.82	1.09	0.68	0.89	0.84	1.17

测试单位: 国家地质实验测试中心, 分析方法: 主量元素为 X 射线荧光光谱(XRF), 微量元素为 ICP-MS; 表中所列的主量元素含量为去除烧失量后的含量, Total 为原始测试数据主量元素总量; 表中 FeO^{T} 代表全铁的含量, $\text{FeO}=\text{FeO}^{\text{T}} \times 0.8998$; $\text{Mg}^{\#}=100 \times \text{Mg}/(\text{Mg}+\text{Fe})$; $\delta\text{Eu}=2\text{Eu}/(\text{Sm}+\text{Gd})$ 。

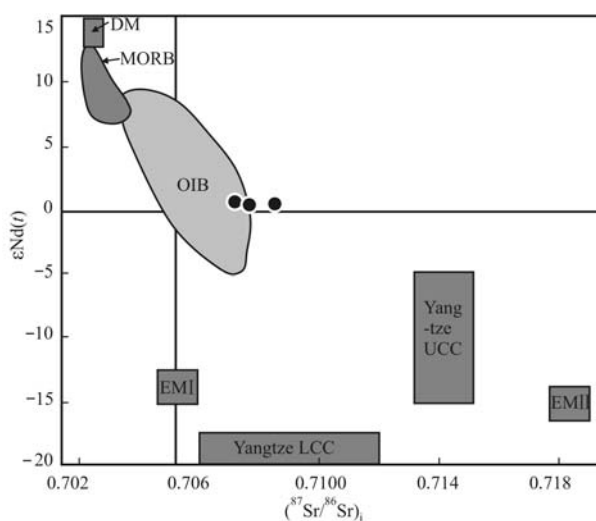
图 7 长界橄榄辉石岩 $\epsilon_{\text{Nd}}(t)$ - $(^{87}\text{Sr}/^{86}\text{Sr})_i$ 图解

Fig. 7 $\epsilon_{\text{Nd}}(t)$ vs. $(^{87}\text{Sr}/^{86}\text{Sr})_i$ diagram of the Changjie olivine pyroxenolite

$t = 700 \text{ Ma}$, 下扬子陆壳(LCC)数据来自 Gao *et al.* (1999), Ma *et al.* (2000) 和 Zhao *et al.* (2010), 上扬子陆壳(UCC)数据来自郝太平 (1993), DM(亏损地幔)、MORB(大洋中脊玄武岩)、OIB(洋岛玄武岩)、EMI(富集地幔 I) 和 EM II(富集地幔 II) 数据来自 Hawkesworth *et al.* (1984), Zindler and Hart (1986), Salters and Hart (1991), Salters and White (1998), Salters and Stracke (2004), Stracke *et al.* (2005), Jackson and Dasgupta (2008)

All the initial isotopic ratios were corrected to 700 Ma. The data of the Yangtze lower continental crust (LCC) are from Gao *et al.* (1999), Ma *et al.* (2000) and Zhao *et al.* (2010), and the data of the Yangtze upper continental crust (UCC) are from Hao Taiping (1993). The data of DM (depleted mantle), MORB (mid-ocean ridge basalt), OIB (ocean island basalt), EM I (enriched mantle of type I) and EM II (enriched mantle of type II) are from Hawkesworth *et al.* (1984), Zindler and Hart (1986), Salters and Hart (1991), Salters and White (1998), Salters and Stracke (2004), Stracke *et al.* (2005), Jackson and Dasgupta (2008)

表 3 湘西通道长界橄榄辉石岩 Sr-Nd 同位素组成
Table 3 Sr and Nd isotopic compositions of Changjie olivine pyroxenolite

样号	CJ14-3	CJ14-6	CJ14-7
$w(\text{Rb})/10^{-6}$	4.05	8.56	4.55
$w(\text{Sr})/10^{-6}$	31.79	38.92	35.85
$w(\text{Sm})/10^{-6}$	1.51	1.22	1.20
$w(\text{Nd})/10^{-6}$	5.39	5.22	5.07
$^{87}\text{Rb}/^{86}\text{Sr}$	0.375 4	0.649 3	0.374 6
$^{87}\text{Sr}/^{86}\text{Sr}$	$0.712\ 316 \pm 9$	$0.713\ 702 \pm 7$	$0.711\ 408 \pm 9$
$^{147}\text{Sm}/^{144}\text{Nd}$	0.169 5	0.141 9	0.141 8
$^{143}\text{Nd}/^{144}\text{Nd}_i$	$0.512\ 526 \pm 9$	$0.512\ 407 \pm 8$	$0.512\ 401 \pm 9$
$(^{143}\text{Nd}/^{144}\text{Nd})_i$	0.511 747	0.511 755	0.511 749
$(^{87}\text{Sr}/^{86}\text{Sr})_i$	0.708 561	0.707 206	0.707 661
$\epsilon_{\text{Nd}}(t)$	0.25	0.41	0.29

使岩浆的 $(\text{La}/\text{Ta})_N$ 值迅速升高, 一般都 > 25 (Lasater and DePaolo, 1997), 长界橄榄辉石岩 $(\text{La}/\text{Ta})_N$ 值基本小于 25, 仅有一个样品 $(\text{La}/\text{Ta})_N$ 值高达 38.1, 指示长界橄榄辉石岩岩浆可能受到轻微的大陸岩石圈地幔物质混染, 或者没有受到大陆岩石圈地幔物质混染。总的来说, 长界橄榄辉石岩形成过程中可能仅受到上地壳物质的混染, 如图 9 所示。

4.2 岩浆源区

长界橄榄辉石岩全碱和硅低而镁铁含量高, 属于亚碱性拉斑玄武岩类岩石(图 5a、5b)。长界橄榄辉石岩具有与 OIB 相似的稀土元素和微量元素配分曲线模式(图 6a、6b), 其 Th/Yb 值为 $0.86 \sim 2.23$, 平均值为 1.47, Hf/Th 值为 $0.66 \sim 1.83$, 平均值为 1.2, 亦与 OIB 相似($\text{Th}/\text{Yb} = 1.85$, $\text{Hf}/\text{Th} = 1.95$; Sun and McDonough, 1989)。另外, 长界橄榄辉石岩的 Sr-Nd 同位素比值也接近 OIB 源区(图 7)。综上所述, 稀土、微量及 Sr-Nd 同位素研究表明通道长界橄榄辉石岩可能起源于与 OIB 相似的地幔源区。

一般认为, OIB 起源于地幔柱(如, 丽江苦橄岩, Morgan, 1971, 1972; Zhang *et al.*, 2006)或者软流圈地幔(Hofmann, 1997; Jahn *et al.*, 1999; Zindler *et al.*, 1984)。研究表明地幔柱成因的岩体规模较大(Hart and Kinloch, 1989; Irvine, 1975), 且地幔柱成因的 OIB 稀土元素含量较高(平均值为 200×10^{-6} , Sun and McDonough, 1989), 通道长界橄榄辉石岩出露面积较小, 而且稀土元素总量很低($\sum \text{REE}$ 为 $25.7 \times 10^{-6} \sim 55.6 \times 10^{-6}$)。此外, 地幔柱活动所引发的一般是短时间内的巨量岩浆作用[如峨眉山大火山岩省(Zhang *et al.*, 2006), 西伯利亚大火山岩省(Czamanske *et al.*, 1998; Kamo *et al.*, 2003)], 根据的前人研究, 本区地幔柱的可能活动时间为 825 Ma(Li, 1999; Li *et al.*, 1999, 2003b, 2010; 张春红等, 2009) 和/或 760 Ma(周继彬, 2006), 本次测年结果获得的通道长界橄榄辉石岩锆石 U-Pb 年龄为 700 Ma 左右, 与区域内可能存在的地幔柱活动时间不符。另外, 作者(未发表数据)根据单斜辉石温压计算, 获得长界橄榄辉石岩形成的温度(约 1300°C)与软流圈地幔的温度相当(1280~1350°C, McKenzie and Bickle, 1988), 也佐证了长界橄榄辉石岩可能起源于软流圈地幔而不是地幔柱。因此, 本文认为长界橄榄辉石岩的岩浆源区可能为软流圈地幔, 其形成很可能与区内新元古代软流圈物质上涌有关。

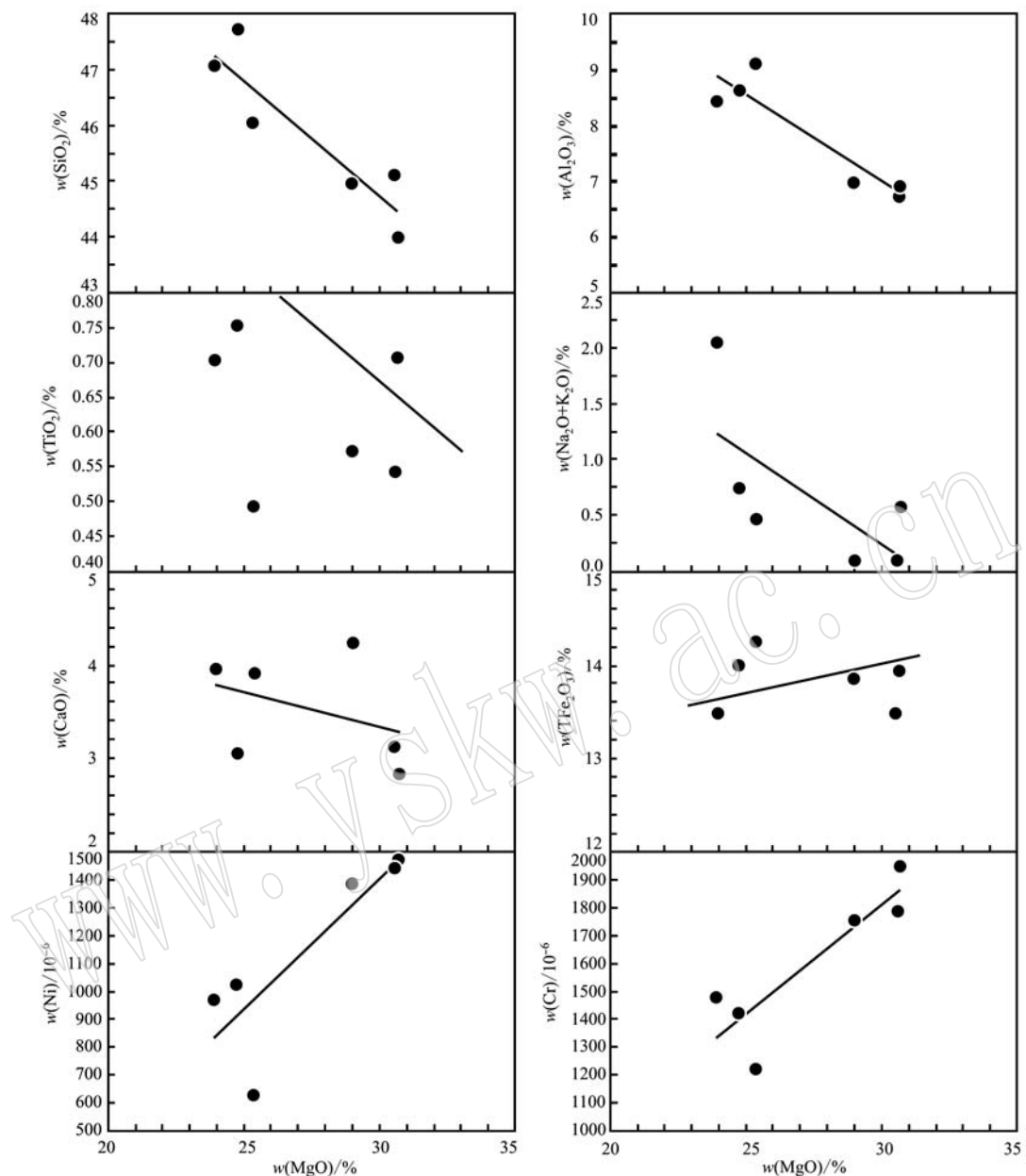


图 8 长界橄榄辉石岩的 MgO 与主要氧化物和一些微量元素的哈克图解

Fig. 8 Variation of MgO versus major and certain trace elements for Changjie olivine pyroxenolite

另外,长界橄榄辉长岩同时还显示出典型“弧岩浆”的特征,如明显的Nb-Ta负异常,较高的Th/Nb值(0.52~0.81)和较低的Nb/La值(0.25~0.44)以及低Nb值(1.1×10^{-6} ~ 3.9×10^{-6}),这些特征均与典型的岛弧玄武岩非常相似(Th/Nb=0.11~2.0,Nb/La=0.15~0.63,Nb平均值为 1.6×10^{-6} ; Kimura and Yoshida, 2006),在Nb/Yb-Th/Yb图(图10a)中,长界橄榄辉石岩也落入MORB-OIB源区上方的岛弧岩浆源区内,Zr/Sm-Nb/Ta图

解(图10b)上也落入弧岩浆内。通常情况下,学者将具有“弧岩浆”特征的OIB解释为受到了地壳物质混染,如桂北元宝山地区超基性岩石和湘西古丈、通道地区辉绿岩(周继斌, 2006; Zhou *et al.*, 2007),如前所述,长界橄榄辉石岩也受到上地壳物质的混染。但是,上地壳的成分主要为长英质,即上地壳物质具有很低的MgO(Xu *et al.*, 2008),如果上地壳物质大量加入到长界橄榄辉石岩岩浆中,长界橄榄辉石岩MgO不可能高达23.97%~30.70%,这说明,

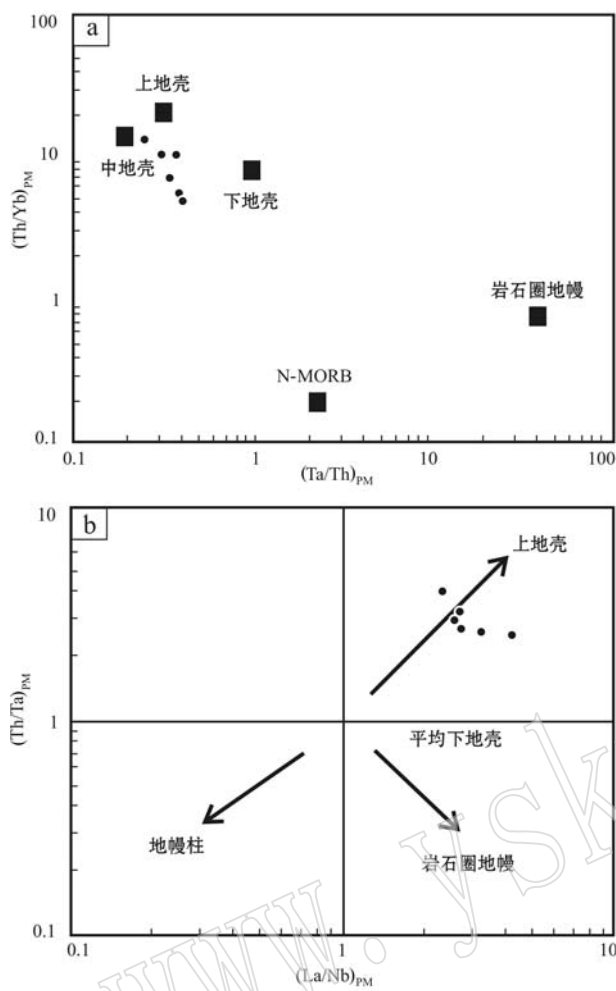


图9 长界橄榄辉石岩 $(\text{Th}/\text{Yb})_{\text{PM}}$ - $(\text{Ta}/\text{Th})_{\text{PM}}$ 图解(a)和 $(\text{Th}/\text{Ta})_{\text{PM}}$ - $(\text{La}/\text{Nb})_{\text{PM}}$ 图解(b, 据Neal *et al.*, 2002)

Fig. 9 Diagram of $(\text{Ta}/\text{Th})_{\text{PM}}$ - $(\text{Th}/\text{Yb})_{\text{PM}}$ (a) and $(\text{Th}/\text{Ta})_{\text{PM}}$ - $(\text{La}/\text{Nb})_{\text{PM}}$ (b, after Neal *et al.*, 2002) for the Changjie olivine pyroxenolite

大陆岩石圈地幔数据来自 McDonough (1990), N-MORB 据 Sun and McDonough(1989), 上、中和下地壳据 Taylor and McLennan (1995)

Data sources: continental lithospheric mantle (McDonough, 1990), N-MORB (Sun and McDonough, 1989), Lower crust, middle crust and upper crust (Taylor and McLennan, 1995)

长界橄榄辉石岩这种“弧岩浆”的特征主要是继承了源区的特征而不是来自地壳混染, 其源区即软流圈地幔可能存在与俯冲作用相关的物质加入, 即在长界橄榄辉石岩形成之前, 在早前俯冲期间该区软流圈地幔可能已经遭受了俯冲流体/熔体的交代作用的改造。研究表明, 扬子板块西缘在新元古代时期曾经是一个活动大陆边缘, 古华南洋板片处于北西方向向扬子板块下部俯冲的构造动力学机制中

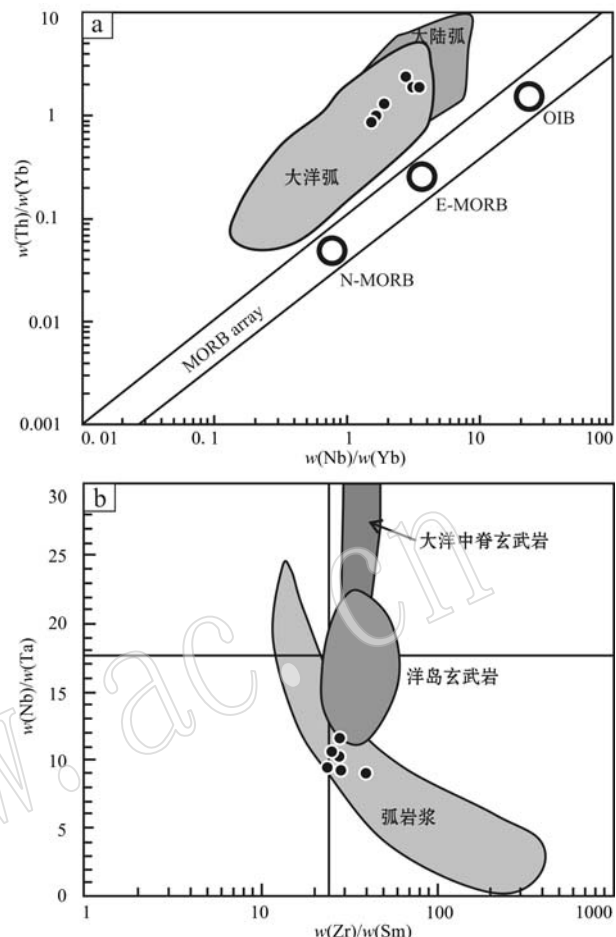


图10 长界橄榄辉石岩 Th/Yb-Nb/Yb 图解(a, 据 Pearce and Peate, 1995) 和 Nb/Ta-Zr/Sm 图解(b, 据 Foley *et al.*, 2000)

Fig. 10 Th/Yb-Nb/Yb diagram (a, after Pearce and Peate, 1995) and Nb/Ta-Zr/Sm diagram (b, after Foley *et al.*, 2000) for the Changjie olivine pyroxenolite

N-MORB—正常的大洋中脊玄武岩; E-MORB—富集的大洋中脊玄武岩; OIB—洋岛玄武岩
N-MORB—normal mid-ocean ridge basalt; E-MORB—enriched mid-ocean ridge basalt; OIB—ocean island basalt

(Yao *et al.*, 2013, 2014), 这可能是源区加入俯冲流体/熔体的主要机制。

综上所述, 本文推测长界橄榄辉石岩的源区是软流圈地幔, 但在形成通道长界橄榄辉石岩之前该区软流圈地幔已经遭受到了来自俯冲消减板片脱水或熔融形成的流体/熔体的交代。

研究表明, 轻稀土元素(LREE)无论是在尖晶石还是石榴子石中都是不相容的, 而重稀土(HREE)在石榴子石中则是相容的, 但在尖晶石中是不相容的(McKenzie and O’Nions, 1991; Irving and Frey,

1984), 较平坦的 HREE 球粒陨石配分曲线暗示长界橄榄辉石岩起源于尖晶石相橄榄岩区 [$(\text{Dy}/\text{Yb})_{\text{N}} = 1.27 \sim 1.56$], 长界橄榄辉石岩低 $(\text{La}/\text{Yb})_{\text{N}}$ 值 ($3.4 \sim 6.5$) 也说明源区为尖晶石残留相 (Yang *et al.*, 2007)。Lassiter 等 (1997) 研究表明, 有些不相容元素因其具有相似的分配系数 (例如 Yb 和 Sm), 故其比值变化很小且不受分离结晶作用的影响, 如 Tb/Yb 和 Yb/Sm , 所以其可以用来指示源区特征及岩浆演化过程。由 $(\text{Tb}/\text{Yb})_{\text{PM}}$ 和 $(\text{Yb}/\text{Sm})_{\text{PM}}$ 图解可知 (图 11), 长界橄榄辉石岩靠近尖晶石二辉橄榄岩相, 说明熔融作用主要发生在尖晶石稳定区域内, 其熔融程度较低约为 $4\% \sim 7\%$, 这与其岩浆规模较小的特点一致。作者 (未发表数据) 根据单斜辉石温压计算, 获得长界橄榄辉石岩的形成压力为较低约为 2.2 GPa , 且岩石岩较低的 $\text{CaO}/\text{Al}_2\text{O}_3$ 值 ($0.35 \sim 0.61$), 也反映其形成压力较低 (Hirose and Kushiro, 1993; Baker and Stolper, 1994)。

根据 McKenzie 等 (1991) 和 Robinson 等 (1998) 的研究, 尖晶石稳定区的深度应小于 $75 \sim 80 \text{ km}$, 所以长界橄榄辉石岩起源于一个相对较浅的软流圈地幔, 反映了该区软流圈地幔上覆的是减薄的岩石圈, 其厚度可能 $< 80 \text{ km}$ 。

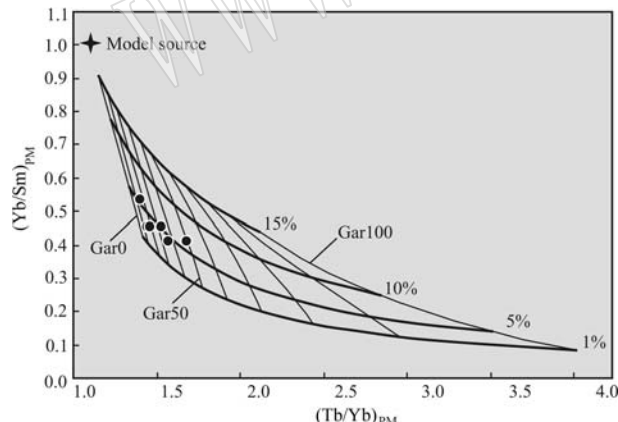


图 11 长界橄榄辉石岩 $(\text{Yb}/\text{Sm})_{\text{PM}} - (\text{Tb}/\text{Yb})_{\text{PM}}$ 图解

Fig. 11 $(\text{Yb}/\text{Sm})_{\text{PM}} - (\text{Tb}/\text{Yb})_{\text{PM}}$ for the Changjie olivine pyroxenolite

据 Shaw, 1970; Janney *et al.*, 2000; Salters and Stracke, 2004; Workman and Hart, 2005; Ito and Mahoney, 2005; Zhang *et al.*, 2006; 格子指示了熔融程度的范围, 熔体在石榴子石相的比例用细线表示, 粗线表示熔体分数

After Shaw, 1970; Janney *et al.*, 2000; Salters and Stracke, 2004; Workman and Hart, 2005; Ito and Mahoney, 2005; Zhang *et al.*, 2006; The grid indicates the range of model compositions. The proportion of melt formed in the presence of garnet is indicated by light lines; curves of constant melt fraction are shown with coarse lines

4.3 深部动力学背景

软流圈物质上涌通常可以通过以下几种方式实现: ① 地幔柱活动 (Wilson, 1989; Zhang *et al.*, 2006); ② 岩石圈拆沉, 即在造山带碰撞晚期, 因重力导致造山带根部坍塌使岩石圈剥离减薄 (Gardien *et al.*, 1997), 从而导致软流圈物质上涌; ③ 俯冲板片的断离使软流圈上涌 (Von Blanckenburg and Davies, 1995); ④ 软流圈地幔对流的热侵蚀作用导致岩石圈减薄 (Houseman *et al.*, 1981) 使软流圈上涌发生熔融; ⑤ 裂谷作用导致软流圈物质上涌, 并发生减压熔融。

如前所述, 长界橄榄辉石岩形成于 700 Ma 左右, 该时期研究区并没有地幔柱活动的证据。在造山带碰撞晚期, 由于重力作用导致岩石圈根部坍塌, 致使岩石圈减薄, 软流圈上涌并发生减压熔融, 与此同时也会导致大规模的地壳熔融 (Turner *et al.*, 1999), 然而, 目前该区并没有报导 700 Ma 时期有大量的壳源岩浆活动。此外, 该区的碰撞造山作用主要发生在 $1100 \sim 850 \text{ Ma}$ 时期 (李江海等, 1999; 陆松年, 2001; 舒良树, 2012), 本次造山作用形成了江南造山带, 岩石圈拆沉通常发生在造山带碰撞晚期, 也就是说, 如果该区发生岩石圈拆沉, 其发生的时间可能为 850 Ma 左右。俯冲板片的断离一般发生在造山带后碰撞时期, 该区在 $850 \sim 800 \text{ Ma}$ 时期处于后碰撞拉伸阶段 (舒良树, 2012)。在对流减薄模型中, 首先发生部分熔融的是岩石圈地幔, 随后是软流圈发生减压熔融。在这种情况下, 由于热源充足, 会形成大规模的岩浆活动 (Turner *et al.*, 1999), 这与本区较小规模的岩浆活动不符合。

综上所述, 形成长界橄榄辉石岩的动力学机制很可能是裂谷作用导致软流圈物质上涌并发生熔融。换言之, 在 700 Ma 时期, 江南造山带西段可能还处于板内裂谷构造背景下, 这与前人的认识一致 (陆松年, 2001; 王孝磊等, 2003; 舒良树, 2012)。McKenzie 等 (1988) 研究表明软流圈发生减压熔融的前提是岩石圈厚度至少要小于 80 km , 即要求软流圈上覆的岩石圈地幔为减薄的岩石圈地幔, 通道长界橄榄辉石岩源区为尖晶石二辉橄榄岩相 ($< 75 \sim 80 \text{ km}$), 符合减薄岩石圈地幔的要求。由此也暗示了 Rodinia 超大陆在 700 Ma 时期仍处于裂解状态。

5 结论

(1) 长界橄榄辉石岩也具有低 SiO_2 ($44.01\% \sim 47.72\%$), 高 MgO ($23.97\% \sim 30.70\%$), 全碱含量

低($\text{Na}_2\text{O} + \text{K}_2\text{O} = 0.07\% \sim 2.04\%$)的特征,岩石属于亚碱性系列拉斑玄武岩类。在岩浆演化的过程中,发生了单斜辉石和橄榄石以及少量斜长石和钛铁氧化物的分离结晶作用。

(2) 长界橄榄辉石岩具有 OIB 和“弧岩浆”的特征。长界橄榄辉石岩源区为尖晶石二辉橄榄岩相($<75 \sim 80 \text{ km}$),是经历了早期俯冲熔体/流体交代改造的软流圈地幔部分熔融的产物。长界橄榄辉石岩可能经历了上地壳物质的混染。

(3) 长界橄榄辉石岩的成岩年龄为 $701 \pm 11 \text{ Ma}$,形成于裂谷构造背景下的软流圈物质上涌。

(4) Rodinia 超大陆在 700 Ma 时期仍处于裂解状态。

致谢 测试分析工作得到中国地质科学院地质研究所、国家地质实验测试中心、南京大学内生金属矿床成矿机制研究国家重点实验室以及中国地质大学(武汉)相关工作人员的大力协助,审稿人为本文修改提出宝贵意见,在此一并致谢!

References

- Baker M B and Stolper E M. 1994. Determining the composition of high-pressure mantle melts using diamond aggregates[J]. *Geochimica et Cosmochimica Acta*, 58: 2 811~2 827.
- Czamanske G K, Gurevitch A B, Fedorenko V, et al. 1998. Demise of the Siberian plume, paleogeographic and paleotectonic reconstruction from the prevolcanic and volcanic record, north-central Siberia [J]. *International Geological Review*, 40: 95~115.
- Druschke P, Hanson A D, Yan Q R, et al. 2006. Stratigraphic and U-Pb SHRIMP Detrital Zircon Evidence for a Neoproterozoic Continental Arc, Central China: Rodinia Implications[J]. *The Journal of Geology*, 114(5): 627~636.
- Faure M, Shu L S, Wang B, et al. 2009. Intracontinental subduction: a possible mechanism for the Early Palaeozoic Orogen of SE China [J]. *Terra Nova*, 21(5): 360~368.
- Foley S F, Barth M G and Jenner G A. 2000. Rutile/melt partition coefficients for trace elements and an assessment of the influence of rutile on the trace element characteristics of subduction zone magmas [J]. *Geochim. Cosmochim. Acta*, 64: 933~938.
- Gao Linzhi, Chen Jun, Ding Xiaozhong, et al. 2011. Zircon SHRIMP U-Pb dating of the tuff bed of Lengjiaxi and Banxi groups, north-eastern Hunan: constraints on the Wuling Movement[J]. *Geological Bulletin of China*, 30: 1 001~1 008(in Chinese with English abstract).
- Gao S, Ling W, Qiu Y, et al. 1999. Contrasting geochemical and Sm-Nd isotopic compositions of Archean metasediments from the Kongling high-grade terrain of the Yangtze craton: evidence for cratonic evolution and redistribution of REE during crustal anatexis[J]. *Geochimica et Cosmochimica Acta*, 63: 2 071~2 088.
- Gardien V, Lardeaux J M and Ledru P. 1997. Metamorphism during late orogenic extension: insights from the French Variscan belt[J]. *Bull. Soc. Geol. Fr.*, 168: 271~286.
- Ge Wenchuan, Li Xianhua, Li Zhengxiang, et al. 2001. Mafic intrusions in Longsheng area: age and its geological implications[J]. *Chinese Journal of Geology*, 36(1): 112~118(in Chinese with English abstract).
- Guo Lingzhi, Shi Yangshen and Ma Ruishi. 1980. The geotectonic framework and crustal evolution of South China[A]. *Scientific Paper on Geology for International Exchange*[C]. Beijing: Geological Publishing House, 109~116(in Chinese with English abstract).
- Guo Lingzhi, Shi Yangshen, Ma Ruishi, et al. 1996. On the meso-neoproterozoic Jiangnan island arc: its kinematics and dynamics[J]. *Geological Journal of Universities*, 2(1): 1~13(in Chinese with English abstract).
- Hao Taiping. 1993. Sm-Nd isotopic ages of Proterozoic metamorphic rocks from the middle sector of the Jinsha River[J]. *Geological Review*, 39: 52~56(in Chinese with English abstract).
- Hart S R and Kinloch E D. 1989. Osmium isotope systematics in Witwater and Bushveld ore deposit[J]. *Economic Geology*, 84(6): 1 651~1 655.
- Hawkesworth C J, Rogers N W, Van Calsteren P W C, et al. 1984. Mantle enrichment processes[J]. *Nature*, 311: 331~335.
- Hirose K and Kushiro I. 1993. Partial melting of dry peridotites at high pressures: Determination of compositions of melts segregated from peridotite using aggregates of diamond[J]. *Earth Planetary Science Letters*, 114: 477~489.
- Hofmann A W. 1997. Mantle geochemistry: the message from oceanic volcanism[J]. *Nature*, 385: 219~229.
- Hoskin P W O. 2005. Trace element composition of hydrothermal zircon and the alteration of Hadean zircon from the Jack Hills, Australia [J]. *Geochimica et Cosmochimica Acta*, 69: 637~648.
- Hoskin P W O and Schaltegger U. 2003. The composition of zircon and igneous and metamorphic petrogenesis[A]. Hanchar J M and Hoskin P W O. *Zircon*[C]. *Rev. Mineral. Geochem.*, 53: 27~62.

- Houseman G A, McKenzie D P and Molnar P. 1981. Convective instability of a thickened boundary layer and its relevance for the thermal evolution of continental convergent belts [J]. *J. Geophys. Res.*, 86: 6 115~6 132.
- Hu Shouxi and Ye Ying. 2006. Questions to “Cathaysia Old Land”, “Cathaysia Block” and “United Yantze-Cathaysia Old Land” of South China Geological[J]. *Journal of China Universities*, 12(4): 432~439(in Chinese with English abstract).
- Irvine T N. 1975. Crystallization sequences in the Muskox intrusion and other layered intrusions-II. Origin of chromitite layers and similar deposits of other magmatic ores[J]. *Geochimica et Cosmochimica Acta*, 39(6): 991~1 020.
- Irving A J and Frey F A. 1984. Trace element abundances in megacrysts and their host basalts: Constraints on partition coefficients and megacrysts genesis[J]. *Geochimica et Cosmochimica Acta*, 48: 1 201~1 221.
- Ito G and Mahoney J J. 2005. Flow and melting of a heterogeneous mantle: 1. Importance to the geochemistry of ocean island and mid-ocean ridge basalts[J]. *Earth and Planetary Science Letters*, 230: 29~46.
- Jackson M G and Dasgupta R. 2008. Compositions of HIMU, EM1, and EM2 from global trends between radiogenic isotopes and major elements in ocean island basalts[J]. *Earth and Planetary Science Letters*, 276: 175~186.
- Jahn B M, Wu F Y, Lo C H, et al. 1999. Crust-mantle interaction induced by deep subduction of the continental crust: geochemical and Sr-Nd isotopic evidence from post-collisional mafic-ultramafic intrusions of the northern Dabie complex, central China[J]. *Chem. Geol.*, 157: 119~146.
- Janney P E, Macdougall J D, Natland J H, et al. 2000. Geochemical evidence from the Pukapuka volcanic ridge system for a shallow enriched mantle domain beneath the South Pacific superswell[J]. *Earth and Planetary Science Letters*, 181: 47~60.
- Kamo S L, Czamanske G K, Amelin Y, et al. 2003. Rapid eruption of Siberian flood-volcanic rocks, coincident with the Permian-Triassic boundary and mass extinction at 251 Ma[J]. *Earth and Planetary Science Letters*, 214: 75~91.
- Kimura J I and Yoshida T. 2006. Contributions of slab fluid, mantle wedge and crust to the origin of Quaternary lavas in the NE Japan [J]. *Journal of Petrology*, 47: 2 185~2 232.
- Lassiter J C and DePaolo D J. 1997. Plume/lithosphere interaction in the generation of continental and oceanic flood basalts: chemical and isotope constraints[A]. Mahoney J J. *Large Igneous Provinces: Continental, Oceanic, and Planetary Flood Volcanism*[C]. Geophysical Monograph 100, American Geophysical Union, 335~355.
- Li Jianghai and Mu Jian. 1999. Tectonic constraints from Chinese cratonic blocks for there construction of Rodinia[J]. *Scientia Geologica Sinica*, 34(3): 259~272(in Chinese with English abstract).
- Li X H. 1999. U-Pb zircon ages of granites from the southern margin of the Yangtze Block: timing of Neoproterozoic Jinning: Orogeny in SE China and implications for Rodinia Assembly[J]. *Precambrian Research*, 97(1): 43~57.
- Li X H, Li W X, Li Z X, et al. 2009. Amalgamation between the Yangtze and Cathaysia Blocks in South China: Constraints from SHRIMP U-Pb zircon ages, geochemistry and Nd-Hf isotopes of the Shuangxiwu volcanic rocks[J]. *Precambrian Research*, 174(1): 117~128.
- Li X H, Li Z X, Zhou H W, et al. 2003b. SHRIMP U-Pb zircon age, geochemistry and Nd isotope of the Guandaoshan pluton in SW Sichuan: Petrogenesis and tectonic significance[J]. *Science in China (Series D)*, 46: 74~83.
- Li X H, Zhu W G, Zhong H, et al. 2010. The Tongde picritic dikes in the western Yangtze Block: Evidence for Ca. 800 Ma mantle plume magmatism in South China during the breakup of Rodinia[J]. *The Journal of Geology*, 118(5): 509~522.
- Li Z X, Li X H, Kinny P D, et al. 1999. The breakup of Rodinia: did it start with a mantle plume beneath South China? [J]. *Earth and Planetary Science Letters*, 173: 171~181.
- Li Z X, Li X H, Kinny P D, et al. 2003a. Geochronology of Neoproterozoic syn-rift magmatism in the Yangtze Craton, South China and correlations with other continents: evidence for a mantle superplume that broke up Rodinia[J]. *Precambrian Research*, 122: 85~109.
- Li Z X, Zhang L H and Powell C M. 1995. South China in Rodinia: part of the missing link between Australia-East Antarctica and Laurentia? [J]. *Geology*, 23(5): 407~410.
- Liu Y S, Gao S, Hu Z C, et al. 2010b. Continental and oceanic crust recycling-induced melt-peridotite interactions in the Trans-North China Orogen: U-Pb dating, Hf isotopes and trace elements in zircons from mantle xenoliths[J]. *Journal of Petrology*, 51: 537~571.
- Liu Y S, Hu Z C, Gao S, et al. 2008. In situ analysis of major and trace elements of anhydrous minerals by LA-ICP-MS without applying an internal standard[J]. *Chemical Geology*, 257: 34~43.
- Liu Y S, Hu Z C, Zong K Q, et al. 2010a. Reappraisal and refine-

- ment of zircon U-Pb isotope and trace element analyses by LA-ICP-MS [J]. Chinese Science Bulletin, 55: 1 535~1 546.
- Lu Songnian. 2001. From Rodinia to Gondwanaland supercontinents—Thinking about problems of researching Neoproterozoic supercontinents[J]. Earth Science Frontiers, 8(4): 441~448(in Chinese with English abstract).
- Ma C Q, Ehlers C, Xu C H, et al. 2000. The roots of the Dabieshan ultrahigh-pressure metamorphic terrane: constraints from geochemistry and Nd-Sr isotope systematics[J]. Precambrian Research, 102: 279~301.
- McDonough W F. 1990. Constraints on the composition of the continental lithospheric mantle[J]. Earth Planetary Science Letters, 101: 1~18.
- McKenzie D and Bickle M J. 1988. The volume and composition of melt generated by extension of the lithosphere[J]. Journal of Petrology, 29: 625~679.
- McKenzie D and O' Nions R K. 1991. Partial melt distributions from inversion of rare earth elements[J]. Journal of Petrology, 32: 1 021~1 091.
- Morgan W J. 1971. Convection plumes in the lower mantle[J]. Nature, 230: 42~43.
- Morgan W J. 1972. Deep mantle convection plumes and plate motions [J]. Petroleum Geologists Bulletin, 2: 203~213.
- Neal C R, Mahoney J J and Chazey W J. 2002. Mantle sources and the highly variable role of continental lithosphere in basalt petrogenesis of the Kerguelen Plateau and Broken Ridge LIP: results from ODP Leg 183[J]. Journal of Petrology, 43: 1 177~1 205.
- Pearce J W and Peate D W. 1995. Tectonic implications of the composition of volcanic arc magmas[J]. Annual Review of Earth and Planetary Sciences, 23: 251~285.
- Polat A, Appel P W U, Fryer B, et al. 2009. Trace element systematics of the Neoarchean Fiskenasset anorthosite complex and associated meta-volcanic rocks, SW Greenland: evidence for a magmatic arc origin[J]. Precambrian Research, 175: 87~115.
- Qi L and Grégoire D C. 2000. Determination of trace elements in twenty-six Chinese geochemistry reference materials by inductively coupled plasma mass spectrometry[J]. Geostandard Newsletter, 24: 51~63.
- Robinson J A and Wood B J. 1998. The depth of the spinel to garnet transition at the peridotite solidus[J]. Earth and Planetary Science Letters, 164: 277~284.
- Salters V J M and Hart S R. 1991. The mantle sources of ocean islands and arc basalts: the Hf isotope connection[J]. Earth and Planetary Science Letters, 104: 364~380.
- Salters V J M and Stracke A. 2004. Composition of the depleted mantle [J]. Geochemistry, Geophysics, Geosystems, 5: 7~27.
- Salters V J M and White W M. 1998. Hf isotope constraints on mantle evolution[J]. Chemical Geology, 145: 447~460.
- Shaw D M. 1970. Trace element fractionation during anatexis[J]. Geochimica et Cosmochimica Acta, 34: 237~243.
- Shu Liangshu. 2012. An analysis of principal features of tectonic evolution in South China Block[J]. Geological Bulletin of China, 31 (7): 1 035~1 053(in Chinese with English abstract).
- Shu L S, Faure M, Yu J H, et al. 2011. Geochronological and geochemical features of the Cathaysia block (South China): New evidence for the Neoproterozoic breakup of Rodinia[J]. Precambrian Research, 187: 263~276.
- Stracke A, Hofmann A W and Hart S R. 2005. FOZO, HIMU, and the rest of the mantle zoo[J]. Geochemistry Geophysics Geosystems, 6, Q05007, doi:10.1029/2004GC000824.
- Sun S S and McDonough W F. 1989. Chemical and isotopic systematics of ocean basalt: implications for mantle composition and processes [J]. Geological Society, London, Special Publications, 42: 313~345.
- Taylor S R and McLennan S M. 1985. The Continental Crust: Its Composition and Evolution[M]. Blackwell: Oxford Press, 312.
- Taylor S R and McLennan S M. 1995. The geochemical composition of the continental crust[J]. Reviews of Geophysics, 33: 241~265.
- Turner S P, Platt J P, George R M M, et al. 1999. Magmatism associated with orogenic collapse of the Betic-Alboran domain, SE Spain [J]. Journal of Petrology, 40: 1 011~1 036.
- Von Blanckenburg F and Davis J H. 1995. Slab breakoff: a model for syncollisional magmatism and tectonics in the Alps[J]. Tectonics, 14: 120~131.
- Wang X L, Zhao G C, Zhou J C, et al. 2008. Geochronology and Hf isotopes of zircon from volcanic rocks of the Shuangqiaoshan Group, South China: Implications for the Neoproterozoic tectonic evolution of the eastern Jiangnan orogen[J]. Gondwana Research, 14: 355~367.
- Wang X L, Zhou J C, Griffin W L, et al. 2014. Geochemical zonation across a Neoproterozoic orogenic belt: Isotopic evidence from granitoids and metasedimentary rocks of the Jiangnan orogen, China[J]. Precambrian Research, 242: 154~171.
- Wang Xiaolei, Zhou Jincheng, Qiu Jiansheng, et al. 2003. Geochem-

- istry of the Meso-Neoproterozoic volcanic-intrusive rocks from Hunan Province and its petrogenetic significances[J]. *Acta Petrologica Sinica*, 19: 49~60(in Chinese with English abstract).
- Wang X L, Zhou J C, Qiu J S, et al. 2004. Geochemistry of the Meso- to Neoproterozoic basic-acid rocks from Hunan Province, South China: implications for the evolution of the western Jiangnan orogen [J]. *Precambrian Research*, 135: 79~103.
- Wang X L, Zhou J C, Qiu J S, et al. 2006. LA-ICP-MS U-Pb zircon geochronology of the Neoproterozoic igneous rocks from Northern Guangxi, South China: Implications for tectonic evolution[J]. *Precambrian Research*, 145: 111~130.
- Wang Yinxi, Gu Lianxing, Zhang Zunzhong, et al. 2007. Sr-Nd-Pb isotope geochemistry of rhyolite of the Late Carboniferous Dashitou Group in eastern Tianshan[J]. *Acta Petrologica Sinica*, 23: 1 749 ~1 755(in Chinese with English abstract).
- Wilson M. 1989. Igneous Petrogenesis[M]. London: Unwin and Hyman.
- Workman R K and Hart S R. 2005. Major and trace element composition of the depleted MORB mantle (DMM) [J]. *Earth and Planetary Science Letters*, 231: 53~72.
- Wu R X, Zheng Y F, Wu Y B, et al. 2006. Reworking of juvenile crust: Element and isotope evidence from Neoproterozoic granodiorite in South China[J]. *Precambrian Research*, 146: 179~212.
- Xia Bin. 1984. A study on geochemical characteristic and emplaced style of two different ophiolites of later Proterozoic Xuefeng stage in the Longsheng regions, Guangxi Southeast China[J]. *Journal of Nanjing University (Natural Sciences)*, 3: 554~566(in Chinese with English abstract).
- Xu Y G, Lan J B, Yang Q J, et al. 2008. Eocene break-off of the Neo-Tethyan slab as inferred from intraplate-type mafic dykes in the Gaoligong orogenic belt, eastern Tibet[J]. *Chemical Geology*, 255: 439~453.
- Xue Huaimin, Ma Fang, Song Yongqin, et al. 2010. Geochronology and geochemistry of the Neoproterozoic granitoid association from eastern segment of the Jiangnanorogen, China: Constraints on the timing and process of amalgamation between the Yangtze and Cathaysia blocks[J]. *Acta Petrologica Sinica*, 26(11): 3 215 ~3 244(in Chinese with English abstract).
- Yan Q R, Hanson A D, Wang Z Q, et al. 2004. Neoproterozoic subduction and rifting on the northern margin of the Yangtze Plate, China: implications for Rodinia reconstruction[J]. *International Geology Review*, 46(9): 817~832.
- Yang J H, Sun J F, Chen F K, et al. 2007. Sources and petrogenesis of late Triassic dolerite dikes in the Liaoning Peninsula: implications for post-collisional lithosphere thinning of the Eastern North China Craton[J]. *J. Petrol.*, 48: 1 973~1 997.
- Yao J L, Shu L S, Santosh M, et al. 2013. Geochronology and Hf isotope of detrital zircons from Precambrian sequences in the eastern Jiangnan Orogen: Constraining the assembly of Yangtze and Cathaysia Blocks in South China[J]. *Journal of Asian Earth Sciences*, 74(2): 225~243.
- Yao J L, Shu L S, Santosh M, et al. 2014. Neoproterozoic arc-related mafic-ultramafic rocks and syn-collision granite from the western segment of the Jiangnan Orogen, South China: Constraints on the Neoproterozoic assembly of the Yangtze and Cathaysia Blocks[J]. *Precambrian Research*, 243: 39~62.
- Yu J H, Wang L J, O'Reilly, et al. 2009. A Paleoproterozoic orogeny recorded in a long-lived cratonic remnant(Wuyishan terrane), eastern Cathaysia Block, China[J]. *Precambrian Research*, 174: 347~363.
- Zhang Chunhong, Fan Weiming, Wang Yuejun, et al. 2009. Geochronology and geochemistry of the Neoproterozoic mafic-ultramafic dykes in the Aikou area, western Hunan Province: Petrogenesis and its tectonic implications[J]. *Geotectonica et Metallogenica*, 33(2): 283~293(in Chinese with English abstract).
- Zhang S B, Zheng Y F, Zhao Z F, et al. 2008. Neoproterozoic anatexis of Archean lithosphere: Geochemical evidence from felsic to mafic intrusions at Xiaofeng in the Yangtze Gorge, South China[J]. *Precambrian Research*, 163: 210~238.
- Zhang Z C, Mahoney J J, Mao J W, et al. 2006. Geochemistry of picroitic and associated basalt flows of the western Emeishan Flood Basalt Province, China[J]. *Journal of Petrology*, 47(10): 1 997~2 019.
- Zhao G C and Cawood P A. 1999. Tectonothermal evolution of the Mayuan Assemblage in the Cathaysia Block: implications for Neoproterozoic collision-related assembly of the South China Craton[J]. *American Journal of Science*, 299(4): 309~339.
- Zhao J H, Zhou M F and Zheng J P. 2010. Metasomatic mantle source and crustal contamination for the formation of the Neoproterozoic mafic dike swarm in the northern Yangtze Block, South China[J]. *Lithos*, 115: 177~189.
- Zheng Y F, Wu R X, Wu Y B, et al. 2008. Rift melting of juvenile arc-derived crust: Geochemical evidence from Neoproterozoic volcanic and granitic rocks in the Jiangnan Orogen, South China[J].

- Precambrian Research, 163: 351~383.
- Zhong J, Chen Y J and Pirajno F. 2016. Geology, geochemistry and tectonic settings of the molybdenum deposits in South China: A review[J]. Ore Geology Reviews, doi: 10.1016/j.oregeorev.2016.04.012.
- Zhou Jibin. 2006. Age and Origin of Neoproterozoic Mafic Magmatism in Northern Guangxi-Western Hunan: In Response to the Break-up of Rodinia? [D]. Chinese Academy of Geological Sciences, Guangzhou (in Chinese with English abstract).
- Zhou J B, Li X H, Ge W C, et al. 2007. Age and origin of middle Neoproterozoic mafic magmatism in southern Yangtze Block and relevance to the break-up of Rodinia[J]. Gondwana Research, 12: 184~197.
- Zhou J C, Wang X L, Qiu J S, et al. 2004. Geochemistry of Meso- and Neoproterozoic mafic-ultramafic rocks from northern Guangxi, China: Arc or plume magmatism? [J]. Geochemical Journal, 38: 139~152.
- Zhou J C, Wang X L and Qiu J S. 2009. Geochronology of Neoproterozoic mafic rocks and sandstones from northeastern Guizhou, South China: Coeval arc magmatism and sedimentation[J]. Precambrian Research, 170: 27~42.
- Zindler A and Hart S R. 1986. Chemical geodynamics[J]. Annual Review of Earth and Planetary Sciences, 14: 493~571.
- Zindler A, Staudigel H and Batiza R. 1984. Isotope and trace element geochemistry of young Pacific seamounts: implication for the scale of upper mantle heterogeneity[J]. Earth Planet. Sci. Lett., 70: 175~195.
- 葛文春, 李献华, 李正祥, 等. 2001. 龙胜地区镁铁质侵入体: 年龄及其地质意义[J]. 地质科学, 36(1): 112~118.
- 郭令智, 卢华夏, 施央申, 等. 1996. 江南中、新元古代岛弧的运动学和动力学[J]. 高校地质学报, 2(1): 1~13.
- 郭令智, 施央申, 马瑞士. 1980. 华南大地构造格架和地壳演化[A]. 26届国际地质大会论文集[C]. 北京: 地质出版社, 109~116.
- 郝太平. 1993. 金沙江中段元古宙变质岩的 Sm-Nd 同位素年龄报道[J]. 地质论评, 39: 52~56.
- 胡受奚, 叶瑛. 2006. 对“华夏古陆”、“华夏地块”及“扬子-华夏古陆统一体”等观点的质疑[J]. 高校地质学报, 12(4): 432~439.
- 李江海, 穆剑. 1999. 我国境内格林威尔期造山带的存在及其对中元古代末期超大陆再造的制约[J]. 地质科学, 34(3): 259~272.
- 陆松年. 2001. 从罗迪尼亞到冈瓦纳超大陆——对新元古代超大陆研究几个问题的思考[J]. 地学前缘, 8(4): 441~448.
- 舒良树. 2012. 华南构造演化的基本特征[J]. 地质通报, 31(7): 1035~1053.
- 王孝磊, 周金城, 邱检生, 等. 2003. 湖南中-新元古代火山-侵入岩地球化学及成因意义[J]. 岩石学报, 19: 49~60.
- 王银喜, 顾连兴, 张遵忠, 等. 2007. 东天山晚石炭世大石头群流纹岩 Sr-Nd-Pb 同位素地球化学研究[J]. 岩石学报, 23: 1749~1755.
- 夏斌. 1984. 广西龙胜元古代二种不同成因蛇绿岩岩石地球化学及侵位方式研究[J]. 南京大学学报, 3: 554~566.
- 薛怀民, 马芳, 宋永勤, 等. 2010. 江南造山带东段新元古代花岗岩组合的年代学和地球化学: 对扬子与华夏地块拼合时间与过程的约束[J]. 岩石学报, 26(11): 3215~3244.
- 张春红, 范蔚茗, 王岳军, 等. 2009. 湘西隘口新元古代基性-超基性岩墙年代学特征: 岩石成因及其构造意义[J]. 大地构造与成矿学, 33(2): 283~293.
- 周继彬. 2006. 桂北-湘西新元古代镁铁质岩的形成时代和成因——对 Rodinia 超大陆裂解的响应[D]. 中国科学院研究生院(广州地球化学研究所).

附中文参考文献

- 高林志, 陈峻, 丁孝忠, 等. 2011. 湘东北岳阳地区冷家溪群和板溪群凝灰岩 SHRIMP 钨石 U-Pb 年龄——对武陵运动的制约[J]. 地质通报, 30: 1001~1008.